



Highly feasible immunoprotective multicistronic SARS-CoV-2 vaccine candidate blending novel eukaryotic expression and *Salmonella* bacterofection



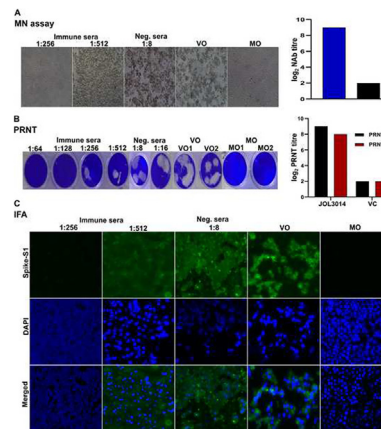
Vijayakumar Jawalagatti, Perumalraja Kirthika, Ji-Young Park, Chamith Hewawaduge, John Hwa Lee*

Department of Veterinary Public Health, College of Veterinary Medicine, Jeonbuk National University, Iksan Campus, 54596, Republic of Korea

HIGHLIGHTS

- P2A enabled multicistronic SARS-CoV-2 vaccine.
- Co-expression of four proteins of SARS-CoV-2.
- *Salmonella* bacterofection-mediated optimum *in vivo* gene delivery.
- Vaccine elicited robust humoral and cellular immune responses.
- Potent neutralizing antibodies against SARS-CoV-2 were recorded.

GRAPHICAL ABSTRACT



ARTICLE INFO

Article history:

Received 28 April 2021

Revised 17 July 2021

Accepted 18 July 2021

Available online 22 July 2021

Keywords:

COVID-19

Vaccine

Salmonella

Multicistronic expression

ABSTRACT

Introduction: The emergence of SARS-CoV-2 variants has raised concerns on future vaccine efficacy as most vaccines target only the spike protein. Hence, vaccines targeting multiple SARS-CoV-2 proteins will offer broader protection and improve our preparedness to combat the pandemic.

Objectives: The study aimed to develop a novel vaccine strategy by combining a eukaryotic vector expressing multiple SARS-CoV-2 genes and *Salmonella*-mediated *in vivo* DNA delivery.

Methods: The eukaryotic vector was designed to function as a DNA-launched RNA replicon in a self-replicating and self-amplifying mRNA mechanism. By exploiting the self-cleaving peptide, P2A, we fused four SARS-CoV-2 targets, including receptor-binding domain (RBD), heptad repeat domain (HR), membrane protein (M) and epitopes of nsp13, in a single open reading frame. Western blot and immunofluorescence assays were used to determine protein expression. In mice, the vaccine's safety and immunogenicity were investigated.

Results: Western blot analysis revealed co-expression all four proteins from the vaccine construct, confirming the efficiency of *Salmonella*-mediated gene delivery and protein expression. The vaccine candidate was safe and elicited robust antigen-specific antibody titers in mice, and a recall response from splenocytes revealed induction of strong cell-mediated immunity. Flow cytometry demonstrated an increase in sub-populations of CD4⁺ and CD8⁺ T cells with the highest CD4⁺ and CD8⁺ T cells recorded for HR and RBD, respectively. Overall, humoral and cellular immune response data suggested the

Peer review under responsibility of Cairo University.

* Corresponding author.

E-mail address: johnhlee@jbnu.ac.kr (J.H. Lee).

<https://doi.org/10.1016/j.jare.2021.07.007>

2090-1232/© 2021 The Authors. Published by Elsevier B.V. on behalf of Cairo University.

This is an open access article under the CC BY-NC-ND license (<http://creativecommons.org/licenses/by-nc-nd/4.0/>).

induction of both Th1 and Th2 immunity with polarization towards an antiviral Th1 response. We recorded a potent SARS-CoV-2 neutralizing antibody titers in the immunized mice sera.

Conclusions: The *Salmonella* bacterofection ensured optimum *in vivo* gene delivery, and through a P2A-enabled efficient multicistronic expression, the vaccine candidate elicited potent anti-SARS-CoV-2 immune responses. These findings provide important insight into development of an effective multivalent vaccine to combat SARS-CoV-2 and its variants.

© 2021 The Authors. Published by Elsevier B.V. on behalf of Cairo University. This is an open access article under the CC BY-NC-ND license (<http://creativecommons.org/licenses/by-nc-nd/4.0/>).

Introduction

Severe acute respiratory syndrome coronavirus 2 (SARS-CoV-2), the etiological agent of coronavirus disease 2019 (COVID-19), prompted a global lockdown in over 220 countries [1]. On February 2021, the World Health Organization (WHO) gave emergency use approval for vaccines such as AstraZeneca/Oxford COVID-19 (ChAdOx1-S) and Pfizer/BioNTech. However, the escalating pandemic and the emergence of novel variants have necessitated the urgent need for multiple vaccines with alternative approaches to achieve equitable global distribution [2]. Most SARS-CoV-2 vaccines target the viral spike protein alone, and mutations in this region that have been detected in variants have raised concerns on future vaccine efficacy [2]. The mutations of greatest concern are located within spike protein regions including in the receptor-binding domain (RBD), furin cleavage site and N-terminal domain. The recently described variant of concern is the B.1.1.7 lineage, which has been dubbed the UK variant [3]. Alarmingly, the variant was found to be more transmissible (75%) than the parent strain [3] with a higher risk of mortality and longer duration of acute infection [4,5]. In March 2021, a difficult-to-diagnose variant was discovered in France, further highlighting the urgent need for alternative ways to halt these variants and their evolution [6]. Hence, multivalent vaccines offering broad protection will be crucial to combat the pandemic. To this end, we have chosen RBD, heptad repeat domain (HR), membrane protein (M) and epitopes of nsp13 of SARS-CoV-2 to design a multivalent vaccine.

To achieve enhanced transgene expression, we designed a eukaryotic vector exploiting the Semliki Forest virus (SFV) replicon, a single-stranded RNA alphavirus that has been widely used in gene therapy applications [7,8]. The SFV replicons were engineered by deleting the genes encoding the structural proteins and replacing them with target genes [9]. The SFV non-structural proteins (nsp1–4) form a replicase complex which is responsible for highly efficient transcription through a self-replicating and self-transcribing mechanism of mRNA [9,10]. However, application of SFV replicons is limited due to the cost intensive virus production and highly transient gene expression. To overcome these challenges, a DNA-launched RNA replicon system was created by replacing the SP6 promoter with the CMV promoter [11] with *Salmonella* bacterofection for *in vivo* delivery.

Taking cues from our experience in the development of *Salmonella*-based vaccines against pathogens of veterinary and medical significance [12–16], we engineered an ST strain with deletions in *lon*, *cpxR*, *rfaL*, *pagL::lpxE* and *asd* named JOL3000. Deletion of the global regulator (*lon*) and stress response regulator (*cpxR*) genes ensures optimum attenuation of ST [17]. One of the major drawbacks of using live-attenuated organisms/vectors for gene therapy is the interference from pre-existing antibodies [18,19]. Therefore, to diminish the impact of pre-existing antibodies on the efficiency of gene delivery and immunogenicity, we deleted O-antigen ligase (*rfaL*) from the ST genome [20]. The replacement of *pagL* (lipid A deacylase) with *lpxE* was made to minimize endotoxicity [21]. *LpxE*

is an inner membrane phosphatase from *Francisella tularensis* when introduced into *Salmonella* leads to the synthesis of 1-monophosphorylated lipopolysaccharide (MPL), which displays low endotoxicity while retaining immunogenicity [21]. Finally, the aspartate-semialdehyde dehydrogenase (*asd*) gene was deleted for antibiotic-free delivery of the vaccine construct [22]. The engineered ST was highly attenuated in mice and retained sufficient invasiveness to ensure the delivery of DNA cargo to target tissues.

The ability of *Salmonella* to invade and proliferate in professional antigen-presenting cells (APCs) such as dendritic cells (DCs) [23] and macrophages [24] makes *Salmonella* an attractive DNA delivery vehicle. Because *Salmonella* can carry large DNA cargo, multiple genes can be cloned in a single vector exploiting viral self-cleaving peptides, such as P2A [25] that will separate large polyprotein into individual proteins. The availability of well-established tools to manipulate the bacterial genome [26] allows the effortless construction of highly safe live-attenuated ST strains and re-engineering ST for tissue specificity. Moreover, *Salmonella* can survive in the host for a relatively long time, which ensures the delivery and expression of a construct for a relatively prolonged period of time compared with conventional DNA/RNA vaccines [27]. Unlike other vaccine platforms, *Salmonella* requires only minimal facilities and resources for vaccine production; thus, large doses of vaccine can be manufactured at an affordable cost. Most importantly, the system can be easily modified with new DNA sequences and provides fast ways to manufacture the vaccine, circumventing tedious processes such as cell culture and other purification techniques. In addition, in the case of emergencies, this bacterium can be easily controlled through the use of antibiotics, which is not possible with replication-competent viral vectors.

We designed a novel vaccine platform by combining eukaryotic expression and *Salmonella*-mediated efficient *in vivo* gene delivery. The aim of the present investigation was to design the multivalent vaccine against SARS-CoV-2 and evaluate its safety and immunogenicity in a mouse model. The current strategy opens a new avenue to combat the ongoing pandemic and presents an alternative way to improve our preparedness to fight the rapidly emerging SARS-CoV-2 variants.

Materials and methods

Mice and ethics statement

Female BALB/c mice, aged five weeks and specific pathogen-free (SPF), were obtained from Koatech in Pyeongtaek, Korea. Mice were maintained on a standard feeding regimen with a 12 h light-dark cycle at the Animal Housing Facility of the College of Veterinary Medicine, Jeonbuk National University. Animal experiments were approved by the Jeonbuk National University Animal Ethics Committee (CBNU2015-00085) under Korean Council on animal care and the Korean Animal Protection Law, 2001, Article 13. The experiments involving live SARS-CoV-2 were carried out at Biosafety Level-3 (BSL3) lab of the Korea Zoonosis Research Institute, South Korea.

Cell lines and virus

HEK293T, Vero E6 and RAW 264.7 cell lines procured from ATCC were maintained in Dulbecco’s modified Eagle’s medium (Lonza, Switzerland) supplemented with 10% fetal bovine serum (Gibco, USA), 100 units/mL penicillin and 100 µg/mL streptomycin at 37 °C in 5% CO₂. Vero E6 cells were used to propagate the SARS-CoV-2 clinical isolate BetaCoV/Korea/KCDC/03/2020 and titers were calculated by a plaque assay. SARS-CoV-2 stocks were stored at –80 °C until further use and passage 3 virus was used in all the experiments.

Bacterial strains, plasmids and primers

Table 1 summarizes the strains of bacteria, plasmids, and primers used in this study. The bacteria were grown in Luria–Bertani broth (LB; BD, USA) with agitation at 37 °C using appropriate antibiotics whenever applicable. For bacterial enumerations, Brilliant Green Agar plates (BD, USA) were used.

Table 1
List of bacterial strains, plasmids and primers used in the present study.

Bacteria/Plasmid	Genotypic characteristics	Reference
S. Typhimurium		
JOL3000	<i>Δlon ΔcpxR Δrfal ΔpagL::lpxE Δasd</i>	Lab stock
JOL3014	JOL3000 carrying pJHL204-V-P2A	This study
JOL3015	JOL3000 carrying pJHL204	This study
<i>E. coli</i>		
DH5α	<i>E. coli</i> F ⁻ Φ80dlacZΔM15Δ (lacZYA-argF) U169recA1 endA1 hsdR17(rk ⁻ , mk ⁺) phoA supE44 thi1 gyr A96 relA1λ ⁻	Lab stock
JOL2606	DH5α carrying pET 28(a) + RBD	This study
JOL2594	DH5α carrying pET 28(a) + HR	This study
JOL2679	DH5α carrying pET 28(a) + M	This study
JOL2612	DH5α carrying pET 28(a) + nsp13	This study
BL21(DE3)	F ⁻ , ompT, hsdS _B (r _B , m _B), dcm, gal, λ (DE3)	Lab stock
JOL2607	DE3 carrying pET 28(a) + RBD	This study
JOL2595	DE3 carrying pET 28(a) + HR	This study
JOL2680	DE3 carrying pET 28(a) + M	This study
JOL2613	DE3 carrying pET 28(a) + nsp13	This study
<i>E.coli</i> 232	F – λ – φ80 Δ(lacZYA-argF) endA1 recA1 hadR17 deoR thi-1 glnV44 gyrA96 relA1 ΔasdA4	Lab stock
JOL3013	<i>E. coli</i> 232 carrying pJHL204-V-P2A	This study
Plasmids		
pET28a(+)	IPTG-inducible expression vector; Kanamycin resistance	Novagen, USA
pSFV3-lacZ	amp ^R , SP6 promoter, pBR322 ori	Addgene, USA
pJHL204	asd ⁺ , CMV promoter, SV40 promoter, pBR322 ori	Lab stock
Protein expression primers		
RBD	Forward – <u>GAATTC</u> AGAGTCCAACCGACTGAA Reverse – <u>AAGCTT</u> GATGATAGACTGAGACGC	This study
HR	Forward – <u>GAATTC</u> ACCAGAACGTACTGTAT Reverse – <u>AAGCTT</u> GGGCCACTTGATATATTG	This study
M	Forward – <u>GAATTC</u> TATTCCGCGTACACGTT Reverse – <u>AAGCTT</u> TGAACCAACAAGCAAT	This study
nsp13	Forward – <u>CCATGG</u> CAACTTACAAATTAATGTTG Reverse – <u>GGATCC</u> AAATATTGTGGCTGTT	This study
Construct primer		
V-P2A	Forward – GGGCCCGCCACCATGAGAGTC Reverse – GCGCGCCTTATATTGTGGCCTG	This study
Cytokine primers		
IFN-γ	Forward – TCAAGTGGCATAGATGTGGAAGAA Reverse – TGCTCTGCGAGATTTTCATG	[71]
TNF-α	Forward – CATCTCTCAAATTCGAGTGACAA Reverse – TGGGAGTAGACAAGGTACAACCC	[71]
IL-4	Forward – ACAGGAGAAGGACGCCAT Reverse – GAAGCCCTACAGACGAGCTCA	[71]
IL-10	Forward – GGTTGCCAAGCCTTATCGGA Reverse – ACCTGCTCCACTGCCTTGCT	[71]
GAPDH	Forward – TCACCACCATGGAGAAGGC Reverse – GCTAAGCAGTTGGTGGTGCA	[71]

Retrieval of SARS-CoV-2 sequences and V-P2A construction

To construct a multi-antigen vaccine, the nucleotide sequences of RBD (756 bp), HR (372 bp), M (666 bp) and selected peptides of RNA-helicase (nsp13, 291 bp) were retrieved from NCBI (NC_045512.2). Each selected antigen was linked using a splicing peptide of 20 amino acids (60 bp) derived from porcine teschovirus-1, P2A and a Kozak consensus sequence was placed at the 5’ end of RBD to enhance translation. The construct was named V-P2A and custom synthesized by Cosmo Genetech, South Korea.

Bioinformatic analysis of the target proteins

The 3D structure of selected SARS-CoV-2 proteins was modelled using Pyhre [28]. The structure refined by Galaxy refine server to minimize distortion [29]. The 3D structure subjected to the PRO-CHECK server for Ramachandran plot analysis as a measure of quality and validation [30] and visualized with Pymol (Schrödinger, LLC; Version 1.2r3pre). Exspasy Protpram online server

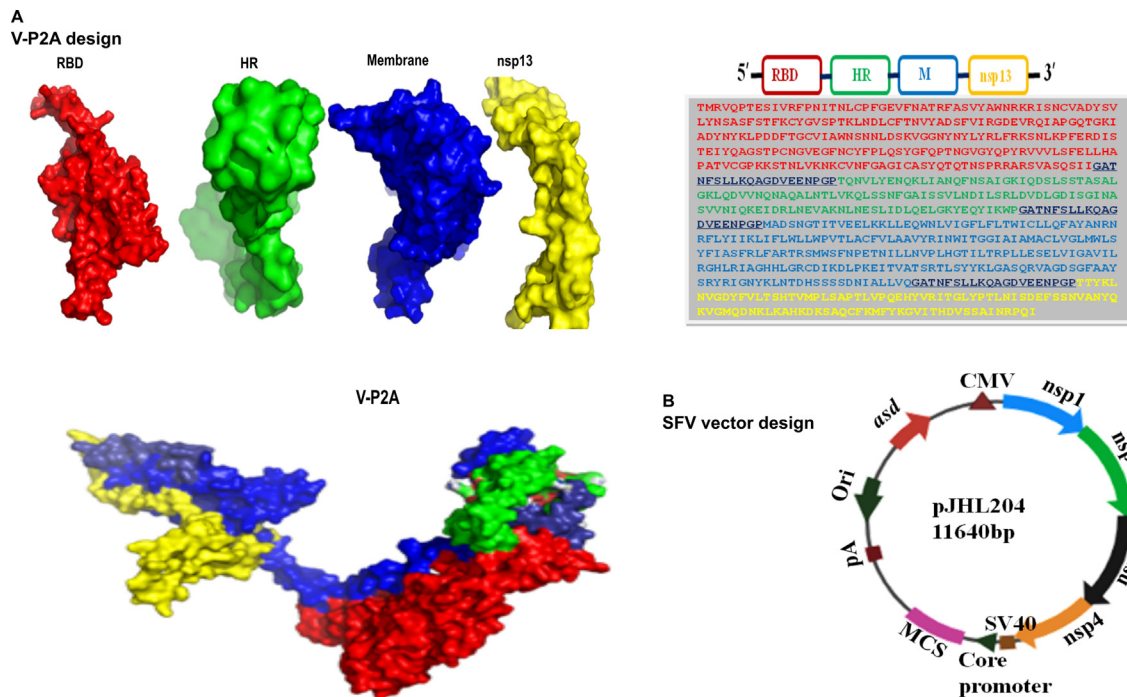


Fig. 1. Construction and characterization of the pJHL204-V-P2A vaccine. (A) The refined 3D models of SARS-CoV-2 proteins and the strategy of vaccine design using P2A peptides is depicted. 3D model of the fusion vaccine construct, V-P2A is shown and indicates the individual components: RBD (red), HR (green), M (blue), nsp13 (yellow) and P2A peptide (deep blue). (B) The SFV replicon vector, pJHL204, is depicted. The CMV promoter, SFV replicase (nsp1–4), SFV sub-genomic core promoter, SV40 promoter, MCS region, polyadenylation signal (pA), asd marker and pBR origin are represented.

(<http://web.expasy.org/protparam>) was applied to determine the physicochemical attributes of proteins. The self-optimized prediction method (SOPMA) was employed to predict secondary conformational states [31]. Additionally, Vaxijen 2.0 server [32] was used to know the antigenicity of proteins. Ellipro servers [33] and BCpred 2 [34] were used to determine the conformational and linear B-cell epitopes, respectively. NetCTL.1.2 server [35] and NetMHCIIpan 3.2 server [36] were used to identify the presence of cytotoxic and helper T cell epitopes.

Vaccine design and construction

We used a SFV replicon-based vector for vaccine construction after making several modifications to pSFV3-lacZ as described in Fig. 1 [11]. Briefly, the SP6 promoter and *lacZ* were replaced with the cytomegalo virus (CMV) promoter and multiple cloning site (MCS) sequences, respectively. MCS comprises the *Apa*I, *Asc*I, *Pac*I, *Asi*SI and *Psi*I restriction sites. Furthermore, to enable antibiotic-free maintenance of the vector, the ampicillin resistance marker was replaced with *asd*, an auxotrophic marker, using *Asc*II and *Sph*I restriction enzymes. The resultant plasmid was designated as pJHL204. The fusion gene was cloned into pJHL204 and the resulting vaccine construct was designated as pJHL204-V-P2A. We used a live-attenuated ST with the genotype *Alon* Δ *cpxR* Δ *rfaL*, *ApagL*::*lpxE* and *Asd*, designated as JOL3000, as the vaccine delivery vehicle. The vaccine strain was prepared by electroporation of JOL3000 with pJHL204-V-P2A. The resulting vaccine strain was designated JOL3014. The vector control strain was prepared by electroporation of JOL3000 with pJHL204 only and the control strain was designated as JOL3015.

Recombinant protein expression and purification and preparation of antibodies

Individual target antigens were expressed in *E. coli* DE3 host using pET28a(+) as a vector. Briefly, the genes were cloned into

pET28a(+) vector following standard directional cloning methods, and the resultant plasmids were used to transform *E. coli* DH5- α strain. After colony PCR confirmation, the recombinant plasmid was extracted and used to transform *E. coli* DE3. The protein expression was induced at 37 °C with 1 mM IPTG for 2–4 h. Following confirmation of protein expression by SDS-PAGE, the protein was purified by Nickel-NTA column chromatography (Takara, Japan) by the urea lysis method. We expressed a truncated M protein of about 14 kDa that consists of major immunodominant epitopes (Supplementary Fig. 3). The selected region comprises 304–666 bp which spans amino acids 102–222 of the C-terminal M protein. The antibodies against individual proteins were raised in rabbits as described elsewhere [37].

Confirming the expression of the vaccine construct

Murine macrophage cells, RAW264.7 in 6-well plates were infected with JOL3014 (pJHL204-V-P2A) at 50 MOI for 3 h. The wells were washed and incubated with 100 μ g/mL gentamycin-containing media to kill the external bacteria for 1 h. After 48 h of incubation, the expression of the vaccine construct was determined by RT-PCR, western blot and IFA. For RT-PCR, RNA was extracted by Trizol method (GeneAll, South Korea) and cDNA was prepared. Expression of full-length construct was confirmed by PCR. The thermal cycling protocol included an initial denaturation at 95 °C for 5 min, followed by 35 cycles of amplification at 30 s and 95 °C for denaturation, 30 s at 54 °C for annealing and 2 min for extension at 72 °C.

To prepare cell lysate for western blotting, 150 μ L RIPA lysis buffer was added to cells and kept on ice for 15 min. Cells were subjected to 2–4 cycles of sonication for 5 s with a 60 s gap at 50% amplitude. The lysate was centrifuged at 10000g for 15 min at 4 °C. The supernatant was mixed with an equal volume 2 \times SDS sample buffer and run on a 12% gel. Samples were transferred to a nitrocellulose membrane (Bio-Rad, USA) and incubated with 3% BSA at room temperature for 2 h to block unsaturated sites. Pri-

mary antibodies raised in rabbits were used at 1:500 dilution and allowed to interact with at 4 °C overnight. The anti-rabbit IgG-HRP antibody at 1:6000 (Southern Biotech, USA) was added and incubated for 1 h at 37 °C. The chromogenic development of membranes was done using DAB substrate and images were documented.

Immunofluorescence assay (IFA) was performed to detect the expression of the vaccine construct using individual rabbit antibodies at 1:200 dilution as described later in the Methods. Cells infected with JOL3015 (vector control) served as negative controls.

Vaccine safety and localization of ST

A group of mice (N = 8) were administered 1×10^7 CFU of the vaccine strain, JOL3014 intramuscularly and monitored for the appearance of any disease symptom, weight loss and mortality for up to 30 days. At 3 and 5 days post-infection, two mice were sacrificed to collect liver and spleen samples. The samples were subjected to histopathological (HP) and IFA analyses to determine the extent of damage and localization of ST, respectively. Quantitative bacterial counts were determined by plating tissue homogenates on BGA agar.

Mouse immunization and sampling

A group of mice (N = 8) were immunized with JOL3014 at a dose of 1×10^7 CFU by intramuscular injection. Another group of mice (N = 8) served as non-immunized controls and were given ST carrying empty vector (JOL3015). A third group of mice (N = 8) did not receive any treatment and served as healthy controls. At three weeks post-immunization, four mice from each group were sacrificed and single cell suspensions of splenocytes were prepared as described previously [38]. Sera samples were collected 3 and 5 weeks following immunization (N = 4). Sera were subjected to heat inactivation at 56 °C for 30 min.

FACS, splenocyte proliferation and cytokine measurement

The splenocytes were cultured in 10% DMEM in a 96-well plate at 1×10^5 cells/well for FACS and splenocyte proliferation assays and in 12-well plate at 1×10^6 cells/well for cytokine measurement. The splenocytes were stimulated with 400 ng of individual recombinant proteins in separate wells for 48 h. To ascertain the changes in T cell populations by FACS, splenocytes were stained with FITC-labeled anti-CD8a, PerCPVio700-labeled anti-CD4 and PE-labeled anti-CD3e antibodies (Miltenyi Biotec, Germany). T-cell subpopulations CD3⁺CD4⁺ and CD3⁺CD8⁺ were gated from CD3⁺ cells and analyzed using the MACSQuant analysis system (Miltenyi Biotec, Germany). Splenocyte proliferation was determined by a standard MTT assay and proliferation index was calculated by dividing A_{570} values from immunized mice with that of control mice. For cytokine measurement, RNA was isolated from splenocytes using a commercial kit (Hybrid-R, GeneAll, South Korea). cDNA was synthesized (Elpis Biotech, South Korea) from 1 µg of purified RNA. Cytokine mRNA levels of TNF- α , IFN- γ , IL-10 and IL-4 were measured using SYBR Green PCR Master Mix (Elpis Biotech, South Korea) and primers listed in Table 1. Thermal cycling conditions were set as pre-incubation at 95 °C for 7 min followed by 40 cycles of 30 s each at 95 °C, 58 °C, and 72 °C. The specificity of the PCR amplification and absence of contamination were confirmed by melting peak analysis with a temperature gradient of 0.1 °C s⁻¹ from 65 °C to 97 °C. Changes in mRNA levels in immunized mice were determined by the $2^{-\Delta\Delta CT}$ method using GAPDH as an internal control [39].

Enzyme-linked immune sorbent assay (ELISA)

End-point antibody titers in mice sera collected at weeks 3 and 5 post-immunization was determined by ELISA. Briefly, 96-well high-binding polystyrene plates (Greiner Bio-One, Austria) were coated with recombinant proteins at 2.5 µg mL⁻¹ in carbonate-bicarbonate buffer, pH 9.6 at 4 °C overnight. The wells were then blocked at 37 °C for 1 h with 200 µL 5% skim milk and washed three times with 0.1% PBST. Serial dilutions of 100 µL sera were added to the wells, and plates were incubated at 37 °C for 1 h and then washed as above. HRP-conjugated goat anti-mouse IgG, IgG1 or IgG2a antibody at 1:5000 or 1:3000 (Southern Biotech, USA) was added and the plates were incubated at 37 °C for 1 h. Finally, following stringent washing, the assay was developed with 100 µL of freshly prepared OPD substrate in phosphate-citrate buffer (pH 5.0) containing H₂O₂ at room temperature for 5–10 min in the dark. The optical densities (OD) were read at 492 nm in a microplate reader (Tecan, Switzerland) after stopping the reaction with 50 µL of 3 M H₂SO₄. The highest serum dilution yielding an absorbance 2.1-fold higher than negative control was recorded as the endpoint titer [40].

Live virus neutralization assays

Microneutralization (MN) assay was carried out as described elsewhere [41]. A 2-fold serial sera dilutions were made and incubated with 200 TCID₅₀ of SARS-CoV-2 at 37 °C for 2 h. Antibody-virus complexes were added onto Vero E6 cell monolayers in 96-well plates and incubated for 72 h. Plates were observed under a microscope for cytopathic effect (CPE) daily for 3 days. Plates were also analyzed by immunofluorescence assay. The highest sera dilution that resulted in complete inhibition of CPE in two of the four wells was recorded as neutralizing antibody titer.

The neutralizing activity was also assessed by plaque reduction neutralization test (PRNT) as described elsewhere [41], with several modifications. A 2-fold serial sera dilutions were incubated with 200 PFU of virus for 2 h at 37 °C. The virus-serum mixtures were added onto Vero E6 cells in a 24-well plate in duplicates and incubated for 1 h at 37 °C in a 5% CO₂ incubator. The monolayers were overlaid with 0.3% agarose (Takara, Japan) in 2% DMEM and the plates were incubated for 5 days. The plates were fixed for 1 h using 10% neutral-buffered formalin (NBF). Following careful removal of the agarose overlay, plates were stained with fixing and staining solution [42]. The maximum dilution causing a 50% (PRNT₅₀) or 90% (PRNT₉₀) reduction in the plaque numbers was identified as an antibody titer.

Immunofluorescence assay (IFA)

IFA was performed to study the replication of SARS-CoV-2 in Vero E6 cells. Briefly, cells were fixed for 10 min with chilled 80% acetone at -20 °C. Cells were permeabilized using 0.1% PBS-Triton X-100 and then blocked with 3% BSA. A 1:500 dilution of SARS-CoV-2 spike S1 primary antibody (Sino Biologicals, China) was added and incubated overnight at 4 °C. After washing, cells were stained with Alexa Fluor 488-conjugated donkey anti-rabbit IgG (Invitrogen, USA) at 1:5000 as a secondary antibody, and DAPI was used to stain the nucleus. Cells were observed under a Leica Fluorescence microscope (Leica Biosystems, Germany).

Statistical analysis

Data analysis was performed by Student's *t* test and repeated measures ANOVA using GraphPad Prism 6.0 software (GraphPad, USA) and IBM SPSS®. A *p*-value < 0.05 was considered significant. Data in graphs are presented as the mean ± SEM with ⁿp > 0.05,

* $p < 0.05$; ** $p < 0.01$; *** $p < 0.001$. The statistical test employed and number of animals is indicated in the figure legends.

Results

In silico analysis of the target proteins

Sequences for RBD, HR, M and nsp13 in SARS-CoV-2 genome were retrieved from National Centre for Biotechnology Information (NCBI). The protein sequences were analyzed in silico using various bioinformatics tools. The refined three dimensional (3D) structures were obtained from the Phyre-2 server; the sequences showed a low percentage of outliers and the Ramachandran plots of the proteins revealed the number of residues located in the favored region (Fig. 1A and Supplementary Fig. S1). The molecular weight, theoretical pI, estimated half-life in human reticulocytes, aliphatic index, grand average of hydropathicity (GRAVY) and antigenicity were observed to be distinct and varied among the proteins (Supplementary Table S1). The predicted secondary structures showed various percentages of α -helices, extended strands, β -turns and random coils (Supplementary Fig. S2). The server-predicted B cell epitopes of the target proteins are listed in Supplementary Table S2 and depicted in Supplementary Fig. S3 and S4. A total of 7 cytotoxic T lymphocyte (CTL) epitopes in RBD, 3 in HR, 10 in M and 4 epitopes in nsp13 were predicted with strong binding affinity. In addition, 3 HTL epitopes in RBD, 3 in HR, 6 in M and 4 epitopes in nsp13 were predicted (Supplementary Table S2).

Construction and characterization of the pJHL204-V-P2A-based vaccine candidate

The SARS-CoV-2 RBD, HR, M and epitopes of nsp13 were fused using a self-cleaving peptide, P2A (V-P2A), and custom synthesized (Fig. 1A). The strategy of using the P2A peptide allows the co-expression of all four SARS-CoV-2 genes from a single open reading frame (ORF) in a coordinated manner. To use the pSFV3-lacZ vector for vaccine construction and expression in eukaryotic cells, the SP6 promoter was replaced with a CMV promoter (Fig. 1B). An MCS sequence was used to replace *lacZ* for directional cloning of target genes. The SV40 promoter was placed just before the SFV sub-genomic core promoter to enable direct nuclear transcription of the vaccine constructs. Importantly, the antibiotic marker was replaced with *asd*, an auxotrophic marker for antibiotic-free cloning and maintenance of the vector. The vector exploits non-structural proteins (nsp) of SFV, named nsp1–4, which through a self-amplifying mechanism lead to enhanced transgene expression [9,10]. The resulting plasmid, pJHL204, was used to clone the target gene resulting in pJHL204-V-P2A. The attenuated ST mutant called JOL3000 was transformed with pJHL204-V-P2A, resulting in the vaccine strain, JOL3014. The JOL3000 strain transformed with pJHL-204 only served as the vector control strain, named JOL3015.

Characterization of protein expression from pJHL204-V-P2A

The expression of the vaccine construct in RAW cells delivered by ST was characterized at mRNA and protein levels. At 48 h post-infection with either the vaccine candidate JOL3014 or the control JOL3015, cell lysates and RNA were prepared. RT-PCR analysis revealed specific amplification of the full-length vaccine construct (2.2 kb) from cDNA from RAW cells infected with JOL3014, whereas no amplification was detected in cells infected with JOL3015 (Supplementary Fig. S5). To characterize the protein expression, western blotting and IFA were carried out using antisera against RBD, HR, M and nsp13 proteins. Western blot in lysates from cells infected with JOL3014 revealed protein bands of 32, 14,

25 and 10 kDa corresponding to the RBD, HR, M and nsp13 proteins, respectively (Fig. 2A). The bright green fluorescence in the cells infected with JOL3014 further confirmed the SARS-CoV-2 proteins expression from the vaccine construct (Fig. 2B). Protein expression was not detected in cells infected with JOL3015. Together, the RT-PCR, western blot and IFA results confirmed the co-expression of all four SARS-CoV-2 antigens from a single ORF.

Assessment of vaccine safety and Salmonella localization

Intramuscular administration of the vaccine strain to mice did not cause any untoward symptoms and no mortality was recorded during the entire experimental period. Importantly, no local lesions, such as ulceration, abscess or necrosis, were observed at the injection site. Histopathological analysis of liver and spleen collected at days 3 and 5 post-infection revealed only minor inflammatory changes with negligible tissue damage (Fig. 3A). A tissue dispersion of red pulp was evident. These changes were absent in the samples collected after two weeks of infection (data not shown).

IFA was carried out to characterize the localization of *Salmonella* in the liver and spleen. Antisera against ST showed the presence of *Salmonella* as fluorescent foci in the liver whereas dispersed fluorescence was noted in the spleen (Fig. 3B). Quantitative bacterial counts were determined by plating tissue homogenates on brilliant green agar plates. An increase in colonization was observed from day 3 to day 5 post-infection and was comparatively higher in the spleen than the liver (Fig. 3C). By day eight, no colonies were recovered from the liver and spleen. Together, these data indicated the excellent safety profile of the *Salmonella*-based vaccination strategy.

Evaluation of vaccine-induced cellular immune response

Mice were immunized with the vaccine strain JOL3014 through the intramuscular route, and a group of mice infected with JOL3015 served as a control. To determine the proliferation index, cytokine profile and changes in the T cell sub-population, 4 mice from each group were sacrificed at week 3 post-immunization. The single cell suspensions of the mouse splenocytes were stimulated with individual recombinant proteins to study the recall response. Changes in the expression profile of transcripts for IFN- γ , TNF- α , IL-4 and IL-10 were evaluated by qPCR. Primer-directed qPCR revealed a significant ($p < 0.05$) upregulation of about 1.9- to 4.84-fold of IFN- γ and 3.3- to 12.9-fold of TNF- α transcripts (Fig. 4A). Similarly, a 2.3- to 4.3-fold increase in IL-10 transcripts was recorded ($p < 0.05$). However, IL-4 transcripts were found to be downregulated upon stimulation with RBD and nsp13 ($p > 0.05$), whereas an upregulation was observed in response to HR ($p > 0.05$) and M proteins ($p > 0.05$). Overall, the upregulation of Th1 cytokines IFN- γ and TNF- α was comparatively higher than that of Th2 cytokines IL-4 and IL-10, suggesting a Th1 polarized immune response.

Flow cytometric determination of immunization-induced changes in T cells revealed a significant increase ($p < 0.05$ – 0.001) in the CD4⁺ and CD8⁺ T cell sub-population compared with the vector controls (Fig. 4B and 4C). The maximum changes in the CD4⁺ T cell population of $5.13 \pm 0.33\%$ was observed in splenocytes stimulated with HR whereas the maximum CD8⁺ T cell population of $1.4 \pm 0.43\%$ was recorded for RBD (Fig. 4C). The mean changes in the CD4⁺ T cells in splenocytes stimulated with RBD, M and nsp13 were 1.85 ± 0.4 , 3.6 ± 0.5 and $2.91 \pm 0.2\%$, respectively. Similarly, the observed mean changes in CD8⁺ T cells in splenocytes stimulated with HR, M and nsp13 were 0.83 ± 0.13 , 0.43 ± 0.06 and $0.25 \pm 0.016\%$, respectively. The mean splenocyte proliferation index recorded for RBD, HR, M and nsp13 was 2.99, 3.44, 3.65 and

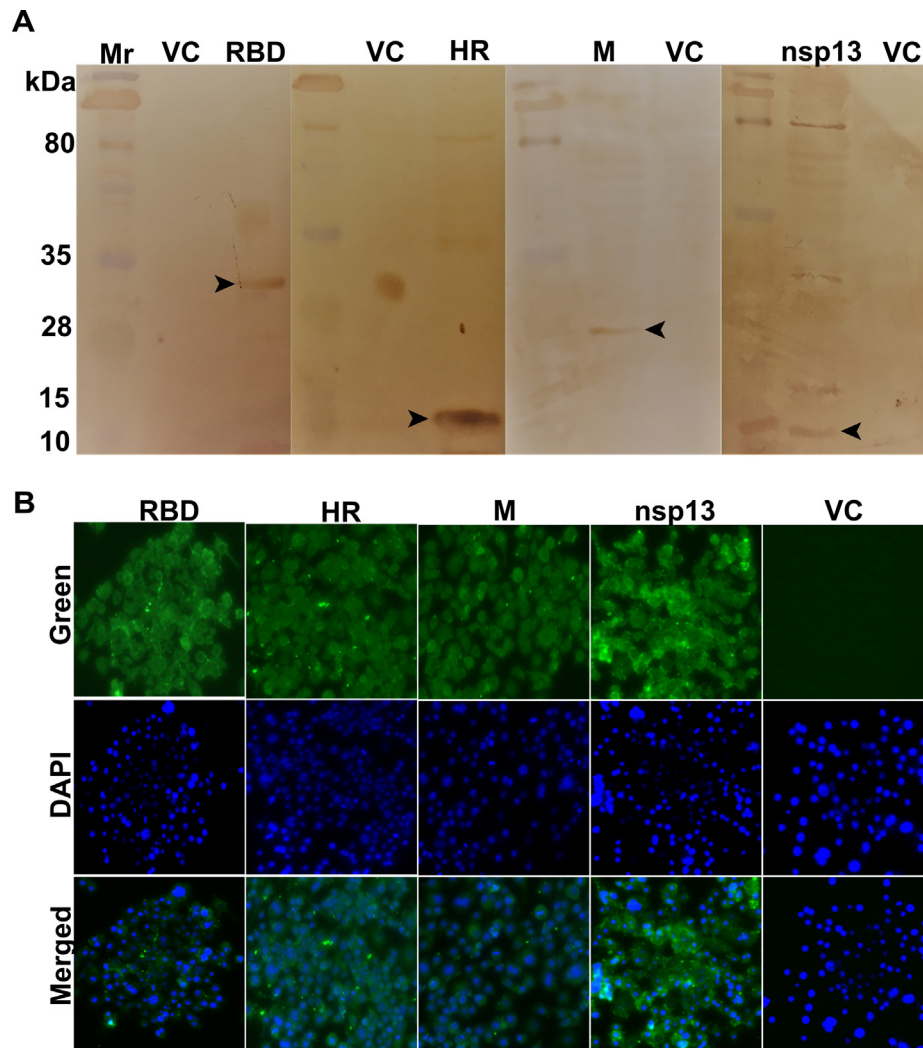


Fig. 2. Characterization of protein expression in RAW cells. The murine macrophage cell line, RAW was infected with the vaccine strain (JOL3014) or, vector control (VC), JOL3015. The protein expression was determined by western blot and IFA. (A) Representative blot image demonstrating the co-expression of proteins. Specific immunoreactivity was detected using antisera against each recombinant protein. Bands of 32, 14, 25 and 10 kDa corresponding to RBD, HR, M and nsp13, respectively, were detected in the lysates of cells infected with JOL3014 but not in the lysates of cells infected with JOL3015. Mr- Protein molecular weight marker. (B) IFA image depicting the expression of proteins in RAW cells. IFA was performed using antisera against each recombinant protein. Bright green fluorescence in JOL3014-infected cells is indicative of protein expression; no such fluorescence was detected in the cells infected with JOL3015.

3.23, respectively (Fig. 4D). Taken together, these data demonstrate the induction of a strong T cell-mediated immune recall response by the vaccine candidate.

Determination of vaccine-elicited antibody titers

The antigen-specific antibody titer in the mouse sera was determined by ELISA using individual recombinant proteins. The sera collected at weeks 3 and 5 post-immunization was analyzed for IgG, IgG1 and IgG2a antibodies. Immunized mice (with JOL3014) mounted an antigen-specific antibody response to all four target proteins (Fig. 5). The mean \log_{10} endpoint titers of RBD-specific IgG, IgG1 and IgG2a were 4.17 ± 0.21 , 4 ± 0.17 and 3.88 ± 0.14 , respectively, at week 3 post-immunization, while the titers for HR protein were 4.48 ± 0.14 , 4.1 ± 0.27 and 4.4 ± 0.21 . Endpoint titers for nsp13 were 3.88 ± 0.144 (IgG), 3.58 ± 0.19 (IgG1) and 4 ± 0.18 (IgG2a). Among the antigen-induced antibody responses, the lowest endpoint titers were recorded for M protein with titers of 3.43 ± 0.18 (IgG), 2.82 ± 0.19 (IgG1) and 3.58 ± 0.14 (IgG2a). Importantly, the immunoglobulin response was maintained at a

similar endpoint titer at week 5 post-immunization with an insignificant increase or decrease in the titer (Supplementary Fig. S6). The order of maximum immunoglobulin titer recorded was HR > RBD > nsp13 > M. Overall, the titer of IgG2a was comparatively higher than that of IgG1, indicating a Th1 dominant immune response. The endpoint \log_{10} antibody titer in vector controls was < 2 for all proteins. These data indicated the highly antigenic nature of the co-expressed proteins, leading to effective stimulation of the humoral response in mice.

Assessment of vaccine-induced neutralizing antibodies

The neutralizing antibodies in mouse sera were evaluated by SARS-CoV-2 neutralization assays. The sera collected at week 3 post-immunization potentially neutralized SARS-CoV-2 with a \log_2 neutralization titer of 9.0, evident by inhibition of CPE in two of the four wells (Fig. 6A). Further, plaque reduction neutralization test (PRNT) revealed PRNT₅₀ and PRNT₉₀ \log_2 antibody titers of 9.0 and 8.0, respectively (Fig. 6B). However, no neutralization was observed in wells treated with vector control sera (Fig. 6A

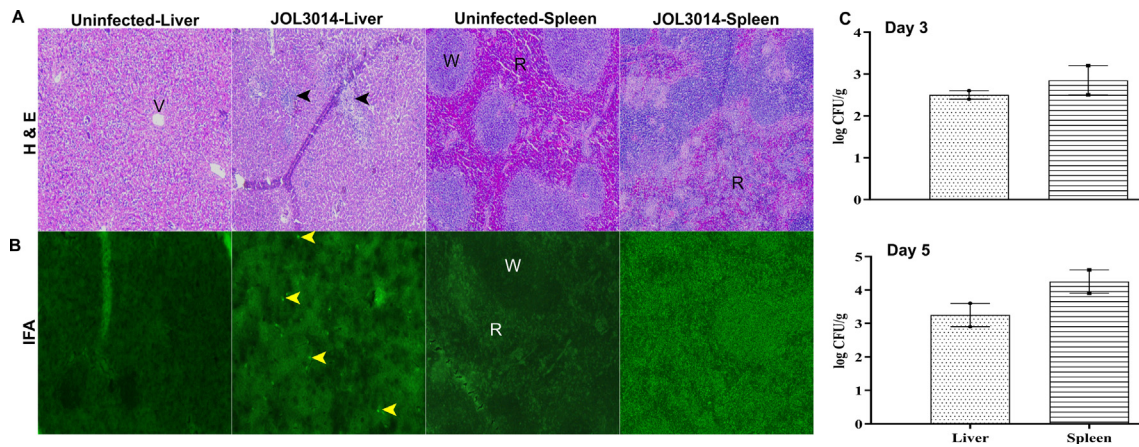


Fig. 3. Assessment of vaccine safety and *Salmonella* localization. Mice (N = 8) were intramuscularly infected with JOL3014 at 1×10^7 CFU. Histopathological changes and *Salmonella* localization in liver and spleen were studied. (A) Haematoxylin and eosin staining of liver and spleen collected at day 5 post-infection. Mild to moderate infiltration of inflammatory cells was observed in liver (black arrowheads). Tissue dispersion of red pulp was observed in spleen. (B) IFA image illustrating the presence of *Salmonella* in liver and spleen at day 5 post-infection. In liver, bacteria were visible as fluorescent foci (yellow arrowheads), whereas in spleen, the fluorescence was dispersed. V, central vein of liver; R, red pulp; W, white pulp. (C) Bar diagram representing quantitative bacterial counts recovered from liver and spleen of mice (N = 2) at days 3 and 5 post-infection with JOL3014. Data presented as mean \pm SEM in log units.

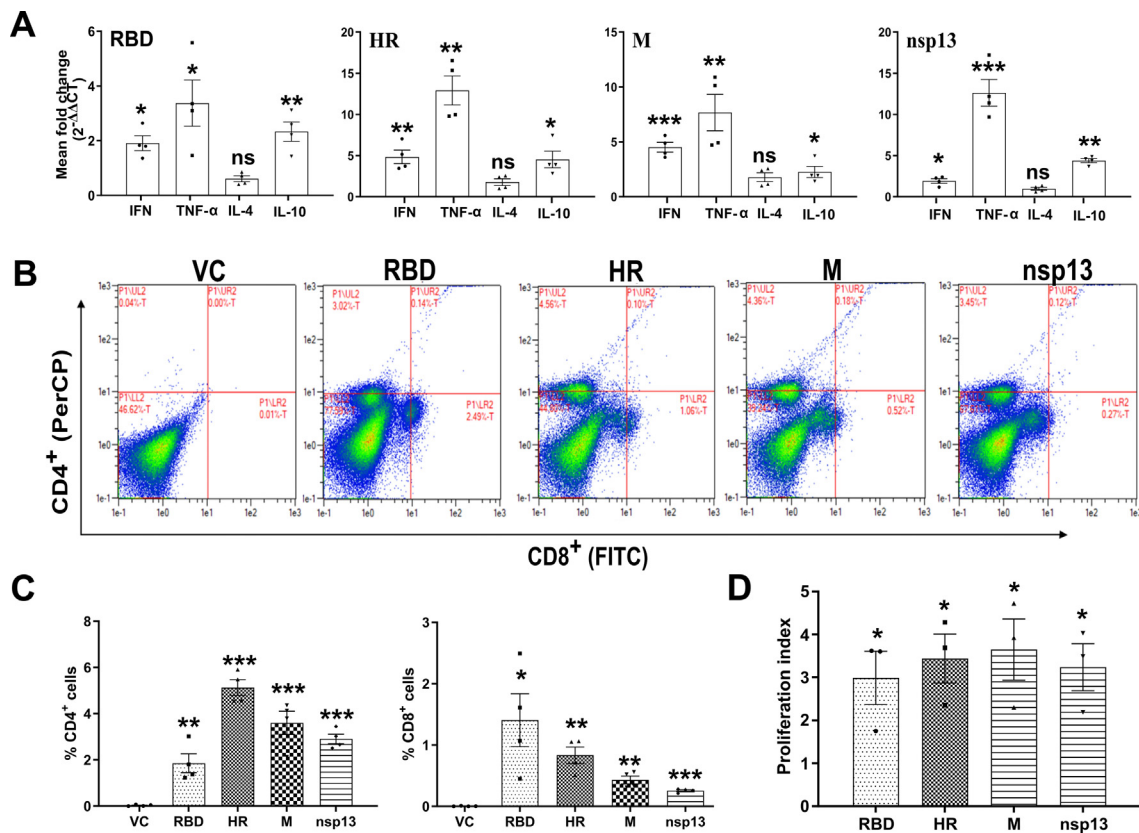


Fig. 4. pJHL204-V-P2A vaccine induces strong cellular immune responses. Immune recall response was analyzed in mice at 3 weeks after immunization. Mice (N = 4) were sacrificed; splenocytes suspension was prepared and stimulated separately with individual recombinant proteins. (A) Changes in the cytokine expression profile of IFN- γ , TNF- α , IL-4 and IL-10 transcripts determined by qPCR at 48 h after stimulation. (B) Representative flow cytometry plots showing changes in sub-populations of CD4⁺ and CD8⁺ T cells. (C) The percentages of CD4⁺ and CD8⁺ T cells were quantified and presented in the bar diagram. (D) Bar diagram showing splenocyte proliferation index. Mice (N = 4) infected with JOL3015 served as vector controls (VC). Data information: Data represent four biologically independent mice per group. In (A, C and D), data represent the individual value from each animal, and the bars reflect the mean values. Error bars denote SEM. Data were analyzed by independent-samples T test and ANOVA. ^{ns} p > 0.05, * p < 0.05, ** p < 0.01 and *** p < 0.001.

and B). These results were corroborated by the observation of inhibition of SARS-CoV-2 replication by S1 spike immunofluorescence assay (Fig. 6C). Collectively, these data suggested the induction of potent SARS-CoV-2 neutralizing antibodies by vaccination.

Discussion

In the present study, we describe the design and development of a novel vaccine platform combining eukaryotic expression and

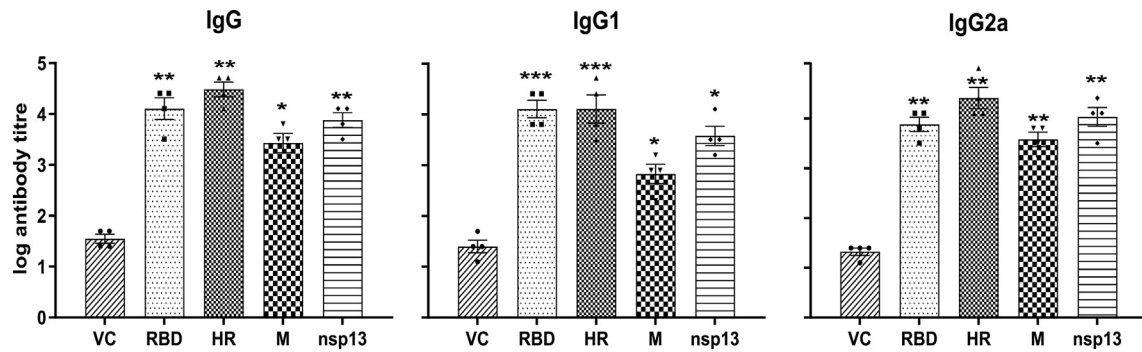


Fig. 5. pJHL204-V-P2A vaccine induces robust antibody responses. Endpoint antibody titer in mouse sera (N = 4) at week 3 post-immunization was determined by ELISA. Antibody titers of IgG, IgG1 and IgG2a are represented from four biologically independent mice per group. Data represent the individual titer of each animal and the bars reflect the means of the titers. Mice infected with JOL3015 served as vector controls (VC). Data are presented in log₁₀ units. Error bars denote SEM. Data were analyzed by independent-samples T test and ANOVA. * p < 0.05, ** p < 0.01 and *** p < 0.001.

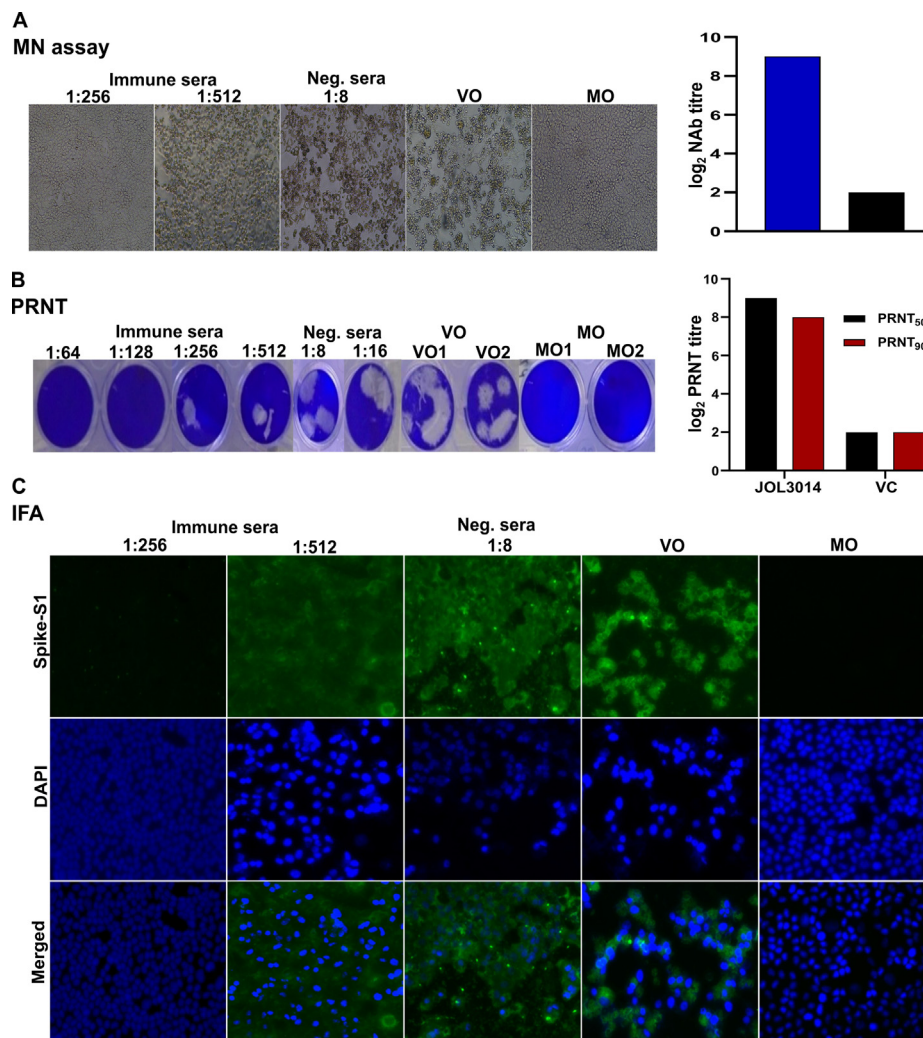


Fig. 6. pJHL204-V-P2A vaccine elicits potent SARS-CoV-2 neutralizing antibodies. Mouse serum collected at week 3 post-immunization was assessed for SARS-CoV-2 neutralizing antibody titer using the Vero E6 cell line. (A) Representative image showing the inhibition of CPE in a microneutralization assay at different sera dilutions. At dilution 512 one of the wells exhibiting CPE is shown (50% inhibition). NAb titer is presented in the right panel. (B) Representative PRNT image illustrating the inhibition of plaque formation in wells treated with immune sera. PRNT₅₀ and PRNT₉₀ titer are presented in the right panel. (C) IFA analysis of neutralization by detecting the expression of spike protein as a measure of viral replication. The degree of green fluorescence is proportional to the viral replication. Data information: The assay was repeated at least twice. NAb and PRNT titers are presented in log₂ units. JOL3014, vaccine strain; VC, vector control (JOL3015); VO, virus only control; MO, medium only control.

Salmonella-mediated gene delivery to combat COVID-19. In 2020–2021 during the global pandemic, we witnessed the development of vaccines at an unprecedented rate. However, the emergence of

new variants has caused concerns over future vaccine efficacy, as most of the currently approved vaccines are based on the spike protein [2]. These variant-derived mutations directly affect the

receptor-binding affinity with an impact on the virulence and transmissibility of SARS-CoV-2 [3,4,43–45]. A hard to diagnose variant was recently discovered in France, further highlighting the urgent need of alternative strategies to halt the evolving variants. Vaccines that target multiple viral proteins will add to the current existing arsenal of COVID-19 prophylactics. With the increasing number of mutations discovered, the development of an efficient vaccine is critical to effectively fight the disease in the near future.

To this end, we chose SARS-CoV-2 proteins such as RBD (spike S1), HR (spike S2), M and nsp13 for the multicistronic vaccine design (Fig. 1A). RBD perceives angiotensin-converting enzyme 2 (ACE2) on host cells and causes conformational changes in the S2 subunit resulting in viral internalization [46]. The role of anti-RBD antibodies in protection has been well established with a strong correlation between neutralizing antibody and RBD-specific ELISA IgG titers [47–52]. The HR domain located within the S2 subunit facilitates the membrane fusion required for viral entry. Upon binding of RBD with ACE2, the HR domain forms a six-helix bundle fusion core to bring viral membrane in close proximity with host cell for fusion and infection [53,54]. Monoclonal antibodies targeting the HR domain were shown to potentially neutralize SARS-CoV-1 [55–57]. Additionally, unlike RBD, the HR domain is highly conserved, and HR antibodies neutralized pseudoviruses expressing different S proteins containing RBD of various clinical isolates [55]. This suggests the suitability of HR-based vaccines to confer protection against a wide range of variants. In one study, an M protein-based vaccine augmented the immune response induced by SARS-CoV nucleocapsid (N), and co-immunization protected Brandt's vole against the challenge infection [58]. Furthermore, highly reactive M protein antibodies were detected in SARS-CoV convalescent sera, and rabbits mounted robust antibody titers against M protein peptides [59]. Results from previous studies on SARS-CoV and the presence of three highly antigenic peptides spanning amino acids 5–20, 180–191 and 199–218 in the SARS-CoV-2 M protein (Supplementary Fig. 3) indicate the inherent antigenic and immunogenic nature of M protein. Consequently, in the current study, M protein was incorporated in the vaccine design to enhance the broader immunity elicited by the vaccine. In addition, selected T cell epitopes of nsp13 were incorporated in the vaccine design to stimulate effective complementary immune responses. The nsp13 encodes an enzyme, RNA-helicase, plays a vital role in viral replication within the replication-transcription complex (RTC) [60]. The nsp13 is highly conserved amongst coronaviruses and represents a promising anti-viral drug target [60]. Vaccines based on non-structural proteins act by activating potent anti-viral T cell responses, particularly CD8⁺ T lymphocytes [61]. Therefore, targeting nsp13 may aid protection through activation of cellular immune responses. The current vaccine candidate encompassing multiple antigens was designed to augment the humoral and cellular immune responses, leading to multitudes of responses and extending improved protection against COVID-19.

We used viral self-cleaving peptide, P2A, from porcine teschovirus-1 to create a SARS-CoV-2 vaccine construct expressing multiple antigens to surmount the limited immune response induced by vaccines comprising a solitary antigen. The viral 2A peptides result in separation of long viral polyproteins into individual proteins without disassembly of the ribosome [25]. Among the several reported viral 2A peptides, P2A was selected because of its high cleavage efficiency [62,63]. By harnessing the self-cleaving feature of P2A, we expressed four SARS-CoV-2 proteins, and the expression of all four proteins was confirmed by western blot and IFA (Fig. 2). Previously, multicistronic expression of three *M. tuberculosis* antigens and a GFP, was achieved by incorporating viral self-cleaving peptides between each protein [64]. Notably, a

cleavage efficiency of 90–100% has been documented in the literature for P2A peptides [62,63]. The results of protein expression and immunogenicity assays demonstrate that the P2A peptide enabled the expression of four SARS-CoV-2 proteins without compromising their expression stability and protein folding.

The limited translation of conventional DNA vectors to humans is a result of the failure of vectors to induce strong immune responses; this can be overcome by SFV vectors that permit enhanced transgene expression [9,10]. To exploit these features of the vector and to overcome the limitations, we designed a DNA-based vaccine construct (Fig. 1B) with *Salmonella* bacteriofection for gene delivery. The engineered ST strain, JOL3000, was highly attenuated in a murine model and exhibited low endotoxicity as assessed by cytokine profile in the infected mice [21]. Moreover, *lpxE* expression in *Salmonella* lessened its virulence in mice by five orders of magnitude without compromising immunogenicity and heterologous antigen delivery [21]. The histopathological analysis of liver and spleen from infected mice showed only minor tissue damage with mild inflammatory cell infiltration, further confirming the excellent safety of ST-mediated gene delivery (Fig. 3A). The vaccine strain was recovered from the liver and spleen of mice for at least five days (Fig. 3C), which ensures the optimal delivery and expression of the construct. Unlike RNA and DNA vaccines, ST does not require the addition of adjuvants, delivery systems or immunomodulators, which minimizes the intricacy and cost of vaccine manufacturing [27]. To elicit humoral response, the antigen does not have to be expressed in a professional APC; however, for a cellular response, the antigen must be formed either within a professional APC or by a cell that can cross-present the antigen [27]. This is one of the major drawbacks of DNA and RNA vaccines, as the uptake of DNA and RNA occurs mostly by non-immune cells [27]. This limitation is effectively overcome by *Salmonella* as it delivers DNA cargo directly to professional APCs, such as macrophages and DCs [23,24], leading to robust T cell responses.

We recorded a mean log₁₀ IgG titer of 3.43 to 4.48 against the different antigens included in the construct (Fig. 5 and Supplementary Fig. 6). Furthermore, the log₂ NAb titer of 9.0 and log₂ PRNT₉₀ titer of 8.0 was recorded against live SARS-CoV-2 (Fig. 6). Previously, the ChAdOx1 nCoV-19 vaccine elicited a log₁₀ IgG titer of 2.66–2.77 with log₂ NAb of 2.3–5.3 [51], while the DNA vaccine elicited a log₂ NAb titer of 6.2–7.4 in immunized monkeys [50]. Consistent with the findings of elicitation of high log₁₀ IgG titer of 5.0 and log₂ NAb titer of 9.84 by the mRNA-RBD vaccine, significant protection was observed against the challenge infection in mice [48]. Furthermore, the NAb titers recorded in our study are comparable to or exceed the NAb titers of convalescent human sera [47,48]. Notably, an inactivated vaccine, although induced a NAb titer of < 1:100, protection was observed against the SARS-CoV-2 challenge [65]. The NAb titer recorded in our study is at least 5-times higher, which would be anticipated to confer protection. Although the correlates of protection are yet to be fully understood, specific memory T cells are likely to extend the long-term protection, suggesting the vital role of cellular immune responses in protection. We observed a strong cellular recall response with significant increases in CD4⁺ and CD8⁺ T cells (Fig. 4), indicating the ability of vaccine to elicit strong cellular responses. The number of M-specific CD4⁺ T cells was relatively higher than that recorded for RBD, suggesting the potential immunodominant nature of M in the induction of CD4⁺ T cells. In a study on COVID-19 patients, a co-dominant CD4⁺ T cell response was observed for spike, M and N proteins and the authors opined that the incorporation of other SARS-CoV-2 structural proteins such as M and N to better mimic the CD4⁺ T cell response observed in natural infection [66]. The observations further indicated the benefits of targeting other antigens, such as M and N, to achieve an optimal vaccine-elicited CD8⁺ responses [66]. One of the pitfalls of vaccines is the

antibody-dependent enhancement (ADE) of disease, which is characterized by a Th2 response [66]. In this study, we observed a Th1 polarized response as indicated by the higher upregulation of pro-inflammatory cytokines like IFN- γ and TNF- α (Fig. 3A). This is corroborated by the humoral response data wherein higher IgG2a titers were recorded in the immunized mice (Fig. 5 and Supplementary Fig. 6). Notably, individuals in the convalescent phase had strong memory T cells despite the absence of detectable SARS-CoV-2 antibodies [67,68], further highlighting the critical role of T cell responses.

We present here a strategy for development of multicistronic vaccine using ST as an optimal delivery vehicle. Due to the lack of animal models to test *S. Typhi*, *S. Typhimurium* serves as a pre-clinical model organism for studies in mice [69]. *S. Typhi* has been validated in humans as a safe and effective vaccine carrier and immunity was documented against heterologous antigens delivered by *S. Typhi* [70]. Importantly, oral route of delivery elicits strong mucosal immune response coupled with humoral and cellular responses, which is desirable for protection against gut and respiratory pathogens, such as SARS-CoV-2 [70]. Therefore, *S. Typhi* may be utilized for human translation after confirming the efficacy of the vaccine in mouse and hamster models of SARS-CoV-2.

Conclusion

In conclusion, this is the first study describing a multicistronic SARS-CoV-2 vaccine combining eukaryotic expression and *Salmonella* bacteriofection. We demonstrate that the *Salmonella* bacteriofection ensured optimum *in vivo* gene delivery, and through a P2A enabled multicistronic expression, the multicistronic vaccine elicited potent anti-SARS-CoV-2 immunity. The candidate exhibits key benefits in the ease of updating DNA sequence and manufacturing large doses of vaccine, which can be achieved in few days. These findings have implications to develop an effective and sustainable vaccine to combat SARS-CoV-2 and its variants.

Compliance with ethics requirements

All animal experiments were performed according to the methods approved by the Jeonbuk National University Animal Ethics Committee (CBNU2015-00085) under the guidelines of the Korean Council on animal care and the Korean Animal Protection Law, 2001, Article 13. All experiments involving handling of live SARS-CoV-2 were carried out at a Biosafety Level-3 (BSL3) lab at the Korea Zoonosis Research Institute, South Korea.

Author contributions

Vijayakumar Jawalagatti: Conceptualization, Investigation, Methodology, Formal Analysis, Writing original draft, review and editing. **Perumalraja Kirthika:** Conceptualization, Investigation, Methodology, Formal Analysis, Writing original draft, review and editing. **Ji-Young Park:** Investigation. **Chamith Hewawaduge:** Investigation. **John Hwa Lee:** Conceptualization, Resources, Funding acquisition, Review and editing.

Declaration of Competing Interest

The authors declare that they have no known competing financial interests or personal relationships that could have appeared to influence the work reported in this paper.

Acknowledgments

This research was supported by Basic Science Research Program through the National Research Foundation of Korea (NRF) funded by the Ministry of Education (2019R1A6A1A03033084).

Data availability

This study includes no data deposited in external repositories.

Appendix A. Supplementary material

Supplementary data to this article can be found online at <https://doi.org/10.1016/j.jare.2021.07.007>.

References

- [1] Shereen MA, Khan S, Kazmi A, Bashir N, Siddique R. COVID-19 infection: Origin, transmission, and characteristics of human coronaviruses. *J Adv Res* 2020;24:91–8.
- [2] Shrotri M, Swinnen T, Kampmann B, Parker EPK. An interactive website tracking COVID-19 vaccine development. *Lancet Glob Heal* 2021;9(5):e590–2.
- [3] Leung K, Shum MHH, Leung GM, Lam TTY, Wu JT. Early transmissibility assessment of the N501Y mutant strains of SARS-CoV-2 in the United Kingdom, October to November 2020. *Eurosurveillance* 2021;26:2002106.
- [4] Kissler SM, Fauver JR, Mack C, Tai C, Breban M, Watkins AE, et al. Densely sampled viral trajectories suggest longer duration of acute infection with B. 1.1. 7 variant relative to non-B. 1.1. 7 SARS-CoV-2. *MedRxiv* 2021.
- [5] Davies NG, Jarvis CI, Edmunds WJ, Jewell NP, Diaz-Ordaz K, Keogh RH, et al. Increased hazard of death in community-tested cases of SARS-CoV-2 Variant of Concern 202012/01. *MedRxiv* 2021.
- [6] Chaqroun A, Hartard C, Schvoerer E. Anti-SARS-CoV-2 vaccines and monoclonal antibodies facing viral variants. *Viruses* 2021;13(6):1171. doi: <https://doi.org/10.3390/v13061171>.
- [7] Komdeur FL, Singh A, van de Wall S, Meulenberg JJM, Boerma A, Hoogbeem BN, et al. First-in-human phase I clinical trial of an SFV-based RNA replicon cancer vaccine against HPV-induced cancers. *Mol Ther* 2021;29(2):611–25.
- [8] Atkins GJ, Smyth JWP, Fleeton MN, Galbraith SE, Sheahan BJ. Alphaviruses and their derived vectors as anti-tumor agents. *Curr Cancer Drug Targets* 2004;4:597–607.
- [9] Liljestrom P, Garoff H. A new generation of animal cell expression vectors based on the Semliki Forest virus replicon. *Bio/Technology* 1991;9(12):1356–61.
- [10] Lundstrom K. Alphaviruses in gene therapy. *Viruses* 2015; 7: 2321–33.
- [11] Kohno A, Emi N, Kasai M, Tanimoto M, Saito H. Semliki Forest virus-based DNA expression vector: transient protein production followed by cell death. *Gene Ther* 1998;5(3):415–8.
- [12] Lalsiamthara J, Lee JH. *Brucella* lipopolysaccharide reinforced *Salmonella* delivering *Brucella* immunogens protects mice against virulent challenge. *Vet Microbiol* 2017;205:84–91.
- [13] Jawale CV, Chaudhari AA, Jeon BW, Nandre RM, Lee JH. Characterization of a novel inactivated *Salmonella enterica* serovar enteritidis vaccine candidate generated using a modified c1857/ PR/gene E expression system. *Infect Immun* 2012;80:1502–9.
- [14] Hyoun KJ, Hajam IA, Lee JH. A consensus-hemagglutinin-based vaccine delivered by an attenuated *Salmonella* mutant protects chickens against heterologous H7N1 influenza virus. *Oncotarget* 2017;8(24):38780–92.
- [15] Kim B, Won G, Lee JH. Construction of an inactivated typhoid vaccine candidate expressing *Escherichia coli* heat-labile enterotoxin B subunit and evaluation of its immunogenicity in a murine model. *J Med Microbiol* 2017;66:1235–43.
- [16] Jawale CV, Lee JH, Waters WR. *Salmonella enterica* serovar enteritidis ghosts carrying the *Escherichia coli* heat-labile enterotoxin B subunit are capable of inducing enhanced protective immune responses. *Clin Vaccine Immunol* 2014;21(6):799–807.
- [17] Kim SW, Moon KH, Baik HS, Kang HY, Kim SK, Bahk JD, et al. Changes of physiological and biochemical properties of *Salmonella enterica* serovar Typhimurium by deletion of *cpxR* and *lon* genes using allelic exchange method. *J Microbiol Methods* 2009;79(3):314–20.
- [18] Mok DZL, Chan KR. The effects of pre-existing antibodies on live-attenuated viral vaccines. *Viruses* 2020;12(5):520. doi: <https://doi.org/10.3390/v12050520>.
- [19] McGhee JR, Roberts M, Bacon A, Li J, Chatfield S. Prior immunity to homologous and heterologous *Salmonella* serotypes suppresses local and systemic anti-fragment C antibody responses and protection from tetanus toxin in mice immunized with *Salmonella* strains expressing fragment C. *Infect Immun* 1999;67(8):3810–5.
- [20] Lalsiamthara J, Kim JH, Lee JH. Engineering of a rough auxotrophic mutant *Salmonella Typhimurium* for effective delivery. *Oncotarget* 2018;9(39):25441–57.

- [21] Kong Q, Six DA, Roland KL, Liu Q, Gu L, Reynolds CM, et al. *Salmonella* synthesizing 1-monophosphorylated lipopolysaccharide exhibits low endotoxic activity while retaining its immunogenicity. *J Immunol* 2011;187(1):412–23.
- [22] Nakayama K, Kelly SM, Curtiss R. Construction of an Asd⁺ expression-cloning vector: stable maintenance and high level expression of cloned genes in a *Salmonella* vaccine strain. *Bio/Technology* 1988;6:693–7.
- [23] Wick MJ. The role of dendritic cells during *Salmonella* infection. *Curr Opin Immunol* 2002;14(4):437–43.
- [24] Gog JR, Murcia A, Osterman N, Restif O, McKinley TJ, Sheppard M, et al. Dynamics of *Salmonella* infection of macrophages at the single cell level. *J R Soc Interface* 2012;9(75):2696–707.
- [25] Sharma P, Yan F, Doronina VA, Escuin-Ordinas H, Ryan MD, Brown JD. 2A peptides provide distinct solutions to driving stop-carry on translational recoding. *Nucleic Acids Res* 2012; 40: 3143–51.
- [26] Datsenko KA, Wanner BL. One-step inactivation of chromosomal genes in *Escherichia coli* K-12 using PCR products. *Proc Natl Acad Sci* 2000;97(12):6640–5.
- [27] Liu MA. A comparison of plasmid DNA and mRNA as vaccine technologies. *Vaccines* 2019;7:37.
- [28] Kelley LA, Mezulis S, Yates CM, Wass MN, Sternberg MJE. The PyMol web portal for protein modeling, prediction and analysis. *Nat Protoc* 2015;10(6):845–58.
- [29] Heo L, Park H, Seok C. GalaxyRefine: Protein structure refinement driven by side-chain repacking. *Nucleic Acids Res* 2013; 41: W384–8.
- [30] Laskowski RA, MacArthur MW, Moss DS, Thornton JM. PROCHECK: a program to check the stereochemical quality of protein structures. *J Appl Crystallogr* 1993;26(2):283–91.
- [31] Geourjon C, Deleage G. SOPMA: Significant improvement in protein secondary structure prediction by c prediction from alignments and joint prediction. *CABIOS* 1995;11:681–4.
- [32] Doytchinova IA, Flower DR. Vaxijen: a server for prediction of protective antigens, tumour antigens and subunit vaccines. *BMC Bioinf* 2007;8:1–7.
- [33] Ponomarenko J, Bui H-H, Li W, Fusseder N, Bourne PE, Sette A, et al. ElliPro: a new structure-based tool for the prediction of antibody epitopes. *BMC Bioinf* 2008;9(1). doi: <https://doi.org/10.1186/1471-2105-9-514>.
- [34] EL-Manzalawy Y, Dobbs D, Honavar V. Predicting linear B cell epitopes using string kernels. *J Mol Recognit An Interdiscip J* 2008;21(4):243–55.
- [35] Larsen MV, Lundegaard C, Lamberth K, Buus S, Lund O, Nielsen M. Large-scale validation of methods for cytotoxic T-lymphocyte epitope prediction. *BMC Bioinf* 2007;8:1–12.
- [36] Jensen KK, Andreatta M, Marcatili P, Buus S, Greenbaum JA, Yan Z, et al. Improved methods for predicting peptide binding affinity to MHC class II molecules. *Immunology* 2018;154(3):394–406.
- [37] Jinyong Z, Xiaoli Z, Weijun Z, Ying G, Gang G, Xuhu M, et al. Fusion expression and immunogenicity of *Bordetella pertussis* PT51-FHA protein: implications for the vaccine development. *Mol Biol Rep* 2011;38(3):1957–63.
- [38] Kruisbeek AM. Isolation of mouse mononuclear cells. *Curr Protoc Immunol* 2000;39:1–3.
- [39] Livak KJ, Schmittgen TD. Analysis of relative gene expression data using real-time quantitative PCR and the 2^{-ΔΔCT} method. *Methods* 2001;25(4):402–8.
- [40] Wu S, Zhong G, Zhang J, Shuai L, Zhang Z, Wen Z, et al. A single dose of an adenovirus-vectored vaccine provides protection against SARS-CoV-2 challenge. *Nat Commun* 2020;11(1). doi: <https://doi.org/10.1038/s41467-020-17972-1>.
- [41] Perera R, Mok CKP, Tsang OTY, Lv H, Ko RL, Wu NC, et al. Serological assays for severe acute respiratory syndrome coronavirus 2 (SARS-CoV-2), March 2020. *Eurosurveillance* 2020;25:2000421.
- [42] Thomas SJ, Nisalak A, Anderson KB, Libraty DH, Kalayanaraj S, Vaughn DW, et al. Dengue plaque reduction neutralization test (PRNT) in primary and secondary dengue virus infections: How alterations in assay conditions impact performance. *Am J Trop Med Hyg* 2009; 81: 825–33.
- [43] Starr TN, Greaney AJ, Addetia A, Hannon WW, Choudhary MC, Dingens AS, et al. Prospective mapping of viral mutations that escape antibodies used to treat COVID-19. *Science* 2021;371(6531):850–4.
- [44] Greaney AJ, Loes AN, Crawford KHD, Starr TN, Malone KD, Chu HY, et al. Comprehensive mapping of mutations in the SARS-CoV-2 receptor-binding domain that affect recognition by polyclonal human plasma antibodies. *Cell Host Microbe* 2021.
- [45] Zekri A-R-N, Amer KE, Hafez MM, Hassan ZK, Ahmed OS, Soliman HK, et al. Genomic characterization of SARS-CoV-2 in Egypt. *J Adv Res* 2020.
- [46] Hoffmann M, Kleine-Weber H, Schroeder S, Krüger N, Herrler T, Erichsen S, et al. SARS-CoV-2 cell entry depends on ACE2 and TMPRSS2 and is blocked by a clinically proven protease inhibitor. *Cell* 2020;181(2):271–280.e8.
- [47] Lau EHY, Tsang OTY, Hui DSC, Kwan MYW, Chan W-H, Chiu SS, et al. Neutralizing antibody titres in SARS-CoV-2 infections. *Nat Commun* 2021;12(1). doi: <https://doi.org/10.1038/s41467-020-20247-4>.
- [48] Huang Q, Ji K, Tian S, Wang F, Huang B, Tong Z, et al. A single-dose mRNA vaccine provides a long-term protection for hACE2 transgenic mice from SARS-CoV-2. *Nat Commun* 2021;12:1–10.
- [49] Mercado NB, Zahn R, Wegmann F, Loos C, Chandrashekar A, Yu J, et al. Single-shot Ad26 vaccine protects against SARS-CoV-2 in rhesus macaques. *Nature* 2020;586(7830):583–8.
- [50] Yu J, Tostanoski LH, Peter L, Mercado NB, McMahan K, Mahrokhian SH, et al. DNA vaccine protection against SARS-CoV-2 in rhesus macaques. *Science* 2020;369(6505):806–11.
- [51] van Doremalen N, Lambe T, Spencer A, Belij-Rammerstorfer S, Purushotham JN, Port JR, et al. ChAdOx1 nCoV-19 vaccine prevents SARS-CoV-2 pneumonia in rhesus macaques. *Nature* 2020;586:578–82.
- [52] Jackson LA, Anderson EJ, Roupael NG, Roberts PC, Makhene M, Coler RN, et al. An mRNA Vaccine against SARS-CoV-2 – Preliminary Report. *N Engl J Med* 2020;383(20):1920–31. doi: <https://doi.org/10.1056/NEJMoa2022483>.
- [53] Bosch BJ, Martina BEE, van der Zee R, Lepault J, Haijema BJ, Versluis C, et al. Severe acute respiratory syndrome coronavirus (SARS-CoV) infection inhibition using spike protein heptad repeat-derived peptides. *Proc Natl Acad Sci* 2004;101(22):8455–60.
- [54] Xia S, Liu M, Wang C, Xu W, Lan Q, Feng S, et al. Inhibition of SARS-CoV-2 (previously 2019-nCoV) infection by a highly potent pan-coronavirus fusion inhibitor targeting its spike protein that harbors a high capacity to mediate membrane fusion. *Cell Res* 2020;30:343–55.
- [55] Elshabrawy HA, Coughlin MM, Baker SC, Prabhakar BS, Pyrc K. Human monoclonal antibodies against highly conserved HR1 and HR2 domains of the SARS-CoV spike protein are more broadly neutralizing. *PLoS ONE* 2012;7(11):e50366.
- [56] Lip K-M, Shen S, Yang X, Keng C-T, Zhang A, Oh H-L, et al. Monoclonal antibodies targeting the HR2 domain and the region immediately upstream of the HR2 of the S protein neutralize in vitro infection of severe acute respiratory syndrome coronavirus. *J Virol* 2006;80(2):941–50.
- [57] Duan J, Yan X, Guo X, Cao W, Han W, Qi C, et al. A human SARS-CoV neutralizing antibody against epitope on S2 protein. *Biochem Biophys Res Commun* 2005;333(1):186–93.
- [58] Shi S, Peng J, Li Y, Qin C, Liang G, Xu L, et al. The expression of membrane protein augments the specific responses induced by SARS-CoV nucleocapsid DNA immunization. *Mol Immunol* 2006;43(11):1791–8.
- [59] He Y, Zhou Y, Siddiqui P, Niu J, Jiang S. Identification of immunodominant epitopes on the membrane protein of the severe acute respiratory syndrome-associated coronavirus. *J Clin Microbiol* 2005;43(8):3718–26.
- [60] White MA, Lin W, Cheng X. Discovery of COVID-19 inhibitors targeting the SARS-CoV-2 Nsp13 helicase. *J Phys Chem Lett* 2020;11(21):9144–51.
- [61] Koup RA, Douek DC. Vaccine design for CD8 T lymphocyte responses. *Cold Spring Harb Perspect Med* 2011; 1: a007252.
- [62] Müntjes K, Philipp M, Hüseman L, Heucken N, Weidtkamp-Peters S, Schipper K, et al. Establishing polycistronic expression in the model microorganism *Ustilago maydis*. *Front Microbiol* 2020;11. doi: <https://doi.org/10.3389/fmicb.2020.01384>.
- [63] Kim JH, Lee S-R, Li L-H, Park H-J, Park J-H, Lee KY, et al. High cleavage efficiency of a 2A peptide derived from porcine teschovirus-1 in human cell lines, zebrafish and mice. *PLoS ONE* 2011;6(4):e18556.
- [64] Mir F-A, Kaufmann SHE, Eddine AN. A multicistronic DNA vaccine induces significant protection against tuberculosis in mice and offers flexibility in the expressed antigen repertoire. *Clin Vaccine Immunol* 2009;16(10):1467–75.
- [65] Gao Q, Bao L, Mao H, Wang L, Xu K, Yang M, et al. Development of an inactivated vaccine candidate for SARS-CoV-2. *Science* 2020;369(6499):77–81.
- [66] Grifoni A, Weiskopf D, Ramirez SI, Mateus J, Dan JM, Moderbacher CR, et al. Targets of T cell responses to SARS-CoV-2 coronavirus in humans with COVID-19 disease and unexposed individuals. *Cell* 2020;181(7):1489–1501.e15.
- [67] Jin P, Li J, Pan H, Wu Y, Zhu F. Immunological surrogate endpoints of COVID-19 vaccines: the evidence we have versus the evidence we need. *Signal Transduct Target Ther* 2021;6:1–6.
- [68] Sekine T, Perez-Potti A, Rivera-Ballesteros O, Strålin K, Gorin J-B, Olsson A, et al. Robust T cell immunity in convalescent individuals with asymptomatic or mild COVID-19. *Cell* 2020;183(1):158–168.e14.
- [69] Santos RL, Zhang S, Tsois RM, Kingsley RA, Garry Adams L, Bäuml AJ. Animal models of *Salmonella* infections: enteritis versus typhoid fever. *Microbes Infect* 2001;3(14–15):1335–44.
- [70] Zhang X-L, Jeza VT, Pan Q. *Salmonella* Typhi: from a human pathogen to a vaccine vector. *Cell Mol Immunol* 2008;5(2):91–7.
- [71] Giulietti A, Overbergh L, Valckx D, Decallonne B, Bouillon R, Mathieu C. An overview of real-time quantitative PCR: applications to quantify cytokine gene expression. *Methods* 2001;25(4):386–401.